

SUPPLEMENTARY INFORMATION FOR

Interbilayer-Crosslinked Multilamellar Vesicles as Synthetic Vaccines for Potent Humoral and Cellular Immune Responses

James J. Moon, Heikyung Suh, Anna Bershteyn, Matthias T. Stephan, Haipeng Liu, Bonnie Huang, Mashaal Sohail, Samantha Luo, Soong Ho Um, Htet Khant, Jessica T. Goodwin, Jenelyn Ramon, Wah Chiu, and Darrell J. Irvine

Correspondence should be addressed to D.J.I. (djirvine@mit.edu)

SUPPLEMENTARY METHODS

Characterization of ICMVs. Particle size and surface charge were determined by dynamic light scattering (DLS) using a 90Plus/ZetaPals particle size and ξ -potential analyzer (Brookhaven Instruments). To quantify the fraction of lipids exposed on the external surfaces of particles, a lamellarity assay was performed as described previously¹. Maleimide and thiol content on the external surface of particles were quantified using fluorimetric quantification kits (ATT Bioquest, Sunnyvale, CA).

Cryoelectron Microscopy. The particles were analyzed using cryoelectron microscopy². A holey carbon-film grid (Quantifoil Micro Tools GmbH, Jena, Germany) was pretreated with Gatan Solarus 950 plasma cleaner. Three μ l of the specimen was applied to the grid, and plunge frozen in liquid ethane using Gatan Cryoplunge 3 (Gatan Inc, Pleasanton, CA, USA). Low dose imaging of the frozen, hydrated specimen kept at liquid nitrogen temperature with a Gatan 626 single tilt cryoholder was performed on a JEM2100 electron microscope (JEOL Ltd, Tokyo, Japan) operating at 200kV. All images were recorded at \sim 40,000x magnification using a Gatan UltraScan 4000 CCD camera.

Thin layer chromatography. To examine crosslinking of maleimide-functionalized lipids, individual lipid components and lipid vesicles before and after interbilayer-crosslinking were dissolved in chloroform, and 5 μ L of the lipids solution was spotted on TLC plate and developed with $\text{CHCl}_3/\text{MeOH}/\text{H}_2\text{O}/\text{NH}_4\text{OH}$ (40:15:2:1). The TLC plate was then dried and visualized with anisaldehyde staining solution.

Synthesis of alkyne-modified lipids and ICMV formation with alkyne-azide chemistry.

744 mg 1,2-dioleoyl-*sn*-glycero-3-phosphoethanolamine (DOPE, 1 mmol) was mixed with

N-hydroxysuccinimide ester of propiolic acid (167 mg, 1 mmol) and Et₃N (202 mg, 2 mmol) in 5 mL CDCl₃, and the reaction was monitored by NMR. After 3 hours at room temperature, the reaction was completed. After the organic solution was washed with 5 mL 5% Na₂CO₃, 1% HCl and brine, dried under Na₂SO₄ and evaporated, alkyne-modified DOPE was weighed. 1.26 μmol of lipid film with DOPC and alkyne-DOPE in 1:1 molar ratio was prepared, hydrated, sonicated, and induced to fuse with 10 mM Mg²⁺ as described previously. MLVs with alkyne-functionalized lipids were incubated with 2.5 mM CuSO₄, copper wire, and 1.5 mM 1, 14-diazido-3,6,9,12-tetraoxatetradecane for 24 hrs at RT. Particle yield was measured after 3X washes with centrifugation.

Incorporation of MPLA in ICMVs. MPLA was incorporated throughout multilayers in ICMVs (int-MPLA ICMVs) by pre-mixing MPLA in lipid film and following the normal synthesis protocol for ICMV and PEGylation. To load MPLA externally on ICMVs (ext-MPLA ICMVs), MPLA was incubated with PEGylated, plain ICMVs for 30 min at 37°C and then washed twice in diH₂O with centrifugation. The incorporation efficiencies of MPLA were 56 ± 2.2% and 14.5 ± 2.3% in int-MPLA and ext-MPLA ICMVs, respectively, as measured with dansyl-modified MPLA. (MPLA was modified with dansylhydrazine as described previously³. Briefly, MPLA was dissolved in 1 mL CHCl₃/MeOH (3:1) with 10 μL TFA, and added with 5 mg of dansylhydrazine (Sigma-aldrich) dissolved in 200 μL EtOH. The reaction mixture was sealed and heated at 70°C for 6 hours. After cooling down to room temperature, the solvent was evaporated under a stream of N₂ and dried under vacuum. The product was washed with cold acetone (3x0.5mL) and purified by silica gel chromatography.) The amount of MPLA added for each method was adjusted to normalize the final amount of MPLA incorporated in ICMVs.

***In vitro* activation study with dendritic cells and CD8⁺ T-cells.**

To examine activation of DCs by ICMVs *in vitro*, we used DCs freshly isolated from spleens of 6-10 wk old C57Bl/6 mice and enriched with an anti-CD11c MACS isolation kit (Stem Cell Technologies, Vancouver, BC, Canada). 4×10^5 splenic DCs were incubated with 0.7 $\mu\text{g/ml}$ of soluble OVA, equivalent doses of OVA loaded in ICMVs, or ICMVs loaded with VMP in the presence or absence of 0.1 $\mu\text{g/ml}$ MPLA. After 18 hrs, cells were analyzed by flow cytometry to examine the extent of DC maturation following staining with anti-CD11c, CD40, CD80, and CD86. To assess the extent of antigen cross-presentation, splenic DCs incubated for 18 hr with 10 $\mu\text{g/mL}$ SIINFEKL peptide (OVA₂₅₇₋₂₆₄), 5.0 $\mu\text{g/mL}$ soluble OVA, equivalent doses of OVA loaded in ICMVs, or VMP-loaded ICMVs in the presence or absence of 0.05 $\mu\text{g/mL}$ MPLA were stained with 25-D1.16 mAb (Ebioscience, San Diego, CA) and analyzed with flow cytometry. Cross-priming of CD8⁺ T-cells by syngeneic splenic DCs was examined *in vitro*. 2×10^4 splenic DCs were pulsed for 4 hrs with 0.7 $\mu\text{g/ml}$ of OVA formulated either in ICMVs or solution with or without 0.1 $\mu\text{g/ml}$ of MPLA, and then co-cultured with 5×10^4 5-(6)-carboxyfluorescein diacetate succinimidyl diester (CFSE)-labeled OVA-specific naïve OT-I CD8⁺ T-cells. After 3 d, proliferation of CD8⁺ T-cells was assessed by flow cytometry analysis of the dilution of CFSE in the OT-I CD8⁺ T-cells.

In some experiments, bone marrow-derived DCs (BMDCs) isolated and cultured as reported previously⁴ were also used to assess activation of DCs. Briefly, bone marrow was isolated from 6-10 wk old C57Bl/6 mice, and the cells were passed through a 70 μm cell strainer, washed, and plated on non-TC Petri dish with 20 ng/ml granulocyte monocyte-colony stimulating factor (GM-CSF) (Peprotech). The culture media was changed on days 3, 6, and 8 with media supplemented with 20 ng/ml GM-CSF. On d10, 4×10^5 BMDCs were incubated with 3.3 $\mu\text{g/ml}$ of OVA loaded in ICMVs with or without addition of 0.36 $\mu\text{g/ml}$ MPLA. After 18 hrs, cells were analyzed by flow cytometry to examine the extent of DC

maturation following staining with anti-CD11c, CD40, CD86, and MHC-II.

Draining of OVA-loaded particles and activation of DCs *in vivo*. Fluorophore-tagged OVA was synthesized by reacting OVA with Alexa Fluor 647-succinimidyl ester (Invitrogen, Carlsbad, CA). C57Bl/6 mice were immunized at tail base s.c. with a single injection of 10 µg fluorophore-tagged OVA and 0.1 µg of MPLA as a soluble, liposomal, or ICMV formulation. After 2 d, draining inguinal lymph nodes were isolated and digested with 100 Mandl U/ml collagenase D for 60 min at RT (Roche, Mannheim, Germany). After passing the lymph node cells through 70 µm cell strainer and washing, the cells were stained with DAPI, anti-CD11c, anti-F4/80, and anti-B220 (Ebioscience) and analyzed with flow cytometry. To examine activation of DCs by ICMV *in vivo*, C57Bl/6 mice were injected at tail base s.c. with 10 µg of OVA mixed with 0.1 µg of MPLA as a soluble, liposomal, or ICMV formulation, and 2 d later, DCs were isolated from draining inguinal lymph nodes and processed to individual cells as mentioned above. After staining the cells with 25-D1.16 mAb, anti-CD11c, anti-CD40, anti-CD86, and anti-MHC-II, they were analyzed with flow cytometry.

SUPPLEMENTARY FIGURE LEGENDS

Supplementary Figure 1. Quenching of available maleimide and thiol groups on the surfaces of ICMVs following DTT treatment and PEG-thiol capping. Percentage of external lipids with **a**, reactive maleimide or **b**, free thiol groups were measured using fluorimetric assays following exposure of MLVs to DTT and PEG-thiol (see Methods). **a**, After interbilayer-crosslinking of Mg^{2+} -fused MLVs with 1.5 mM DTT, the resulting ICMVs had less than 3% of lipids with reactive maleimide groups, which decreased further with subsequent PEG-thiol treatment. **b**, Percentage of external lipids with thiol groups remained minimal (< 0.05 %) during ICMV synthesis, indicating absence of DTT-lipid conjugates with unreacted thiol groups on the external surfaces of ICMVs.

Supplementary Figure 2. CryoEM images of ICMVs. **a-d**, Additional representative cryo-EM images show examples of the thick, multilayered lipid walls formed in ICMVs. Arrow in **d** highlights an example of incomplete external lipid layers seen infrequently in ICMV vesicles. Scale bars = 100 nm.

Supplementary Figure 3. Thin layer chromatography analysis of the crosslinked lipids in ICMVs. Migration patterns of lipids from interbilayer-crosslinked ICMVs were compared to those of non-crosslinked Mg^{2+} -fused liposomes (MLVs) and the individual lipid components (see Supplementary Methods). Arrow at right highlights the position of a unique band seen in lane 4 shifted from the position of monomeric MPB lipids, suggesting successful conjugation of maleimide-functionalized lipids with the dithiol crosslinker.

Supplementary Figure 4. Structures of alternative dithiol crosslinkers tested for ICMV synthesis (cited in Table 2).

Supplementary Figure 5. Alternative interbilayer-crosslinked reaction using “click” chemistry. **a**, An alkyne-headgroup lipid was synthesized from DOPE and an alkyne precursor (see Supplementary Methods). **b**, Liposomes were formed with alkyne-terminated lipids and induced to form MLVs by Mg^{2+} . Subsequent incubation of the alkyne-bearing MLVs with diazide and catalyst as indicated led to successful formation of ICMVs with 83% particle yield, as measured after particle retrieval with low-speed centrifugation conditions.

Supplementary Figure 6. Proteins encapsulated in ICMVs do not undergo chemical modification. To assess the stability of the disulfide linkages in encapsulated proteins, ICMVs loaded with a monoclonal rat IgG antibody were lysed with Triton X-100, and the recovered protein was analyzed by SDS-PAGE under non-reducing conditions. The untreated stock antibody (mAb) showed a major band near 150 kDa, while antibody treated with 10 mM DTT for 30 min (mAb + DTT) showed nearly complete reduction into heavy (50 kDa) and light chain (25 kDa) components. In contrast, IgG recovered from ICMVs was indistinguishable from the unmodified starting material, suggesting that proteins do not undergo significant chemical modification or aggregation during encapsulation in ICMVs.

Supplementary Figure 7. Stimulation of bone marrow-derived DCs by ICMVs supplemented with the TLR agonist MPLA. Bone marrow-derived DCs (BMDCs) were incubated for 18 hr with 3.3 $\mu\text{g}/\text{ml}$ of OVA in ICMVs in the presence or absence of 0.36 $\mu\text{g}/\text{mL}$ MPLA, and the expression levels of the cell surface costimulatory markers (CD40 and CD86) and MHC-II were analyzed with flow cytometry.

Supplementary Figure 8. *In vivo* stimulation of DCs by ICMVs mixed with MPLA.

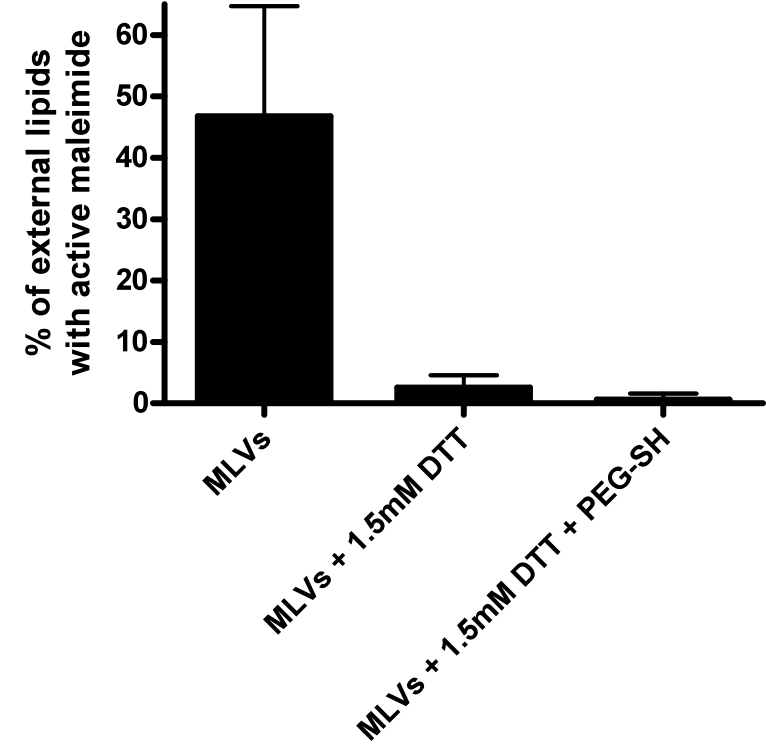
C57Bl/6 mice were injected with 10 µg of OVA mixed with 0.1 µg of MPLA as a soluble, liposomal, or ICMV formulation, and 2 d later, DCs isolated from draining inguinal LNs were analyzed with flow cytometry for costimulation markers (CD40 and CD86) and MHC-II.

SUPPLEMENTARY REFERENCES

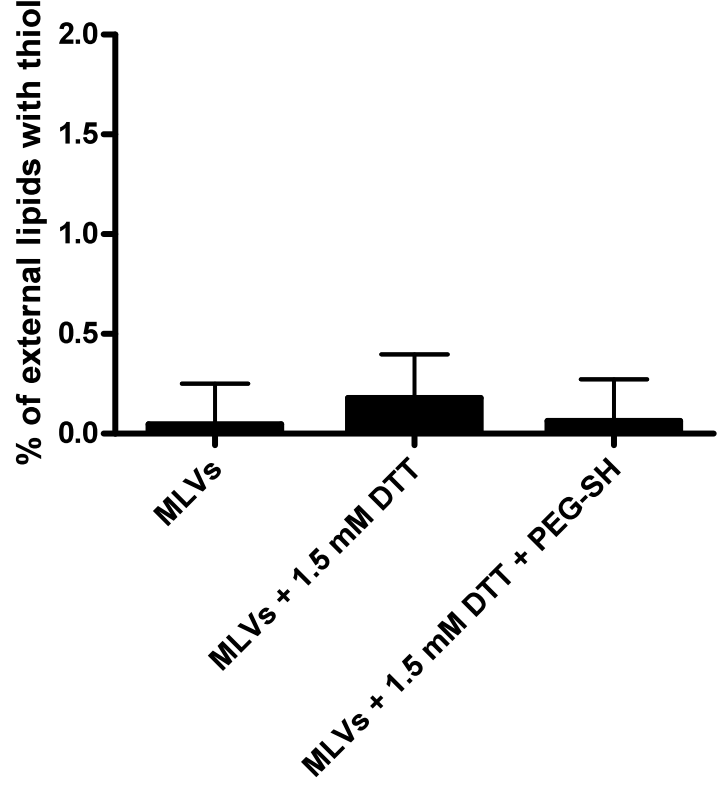
1. Girard, P. et al. A new method for the reconstitution of membrane proteins into giant unilamellar vesicles. *Biophys. J.* **87**, 419-429 (2004).
2. Baker, M. L., Marsh, M. P. & Chiu, W. *Nanotechnology: Cryo-EM of molecular nanomachines and cells*. (Wiley VCH, Weinheim, 2009).
3. Shilova, N. V. & Bovin, N. V. Fluorescent labels for the analysis of mono- and oligosaccharides. *Russian Journal of Bioorganic Chemistry* **29**, 309-324 (2003).
4. Lutz, M. B. et al. An advanced culture method for generating large quantities of highly pure dendritic cells from mouse bone marrow. *J. Immunol. Methods* **223**, 77-92 (1999).

Sup. Fig. 1

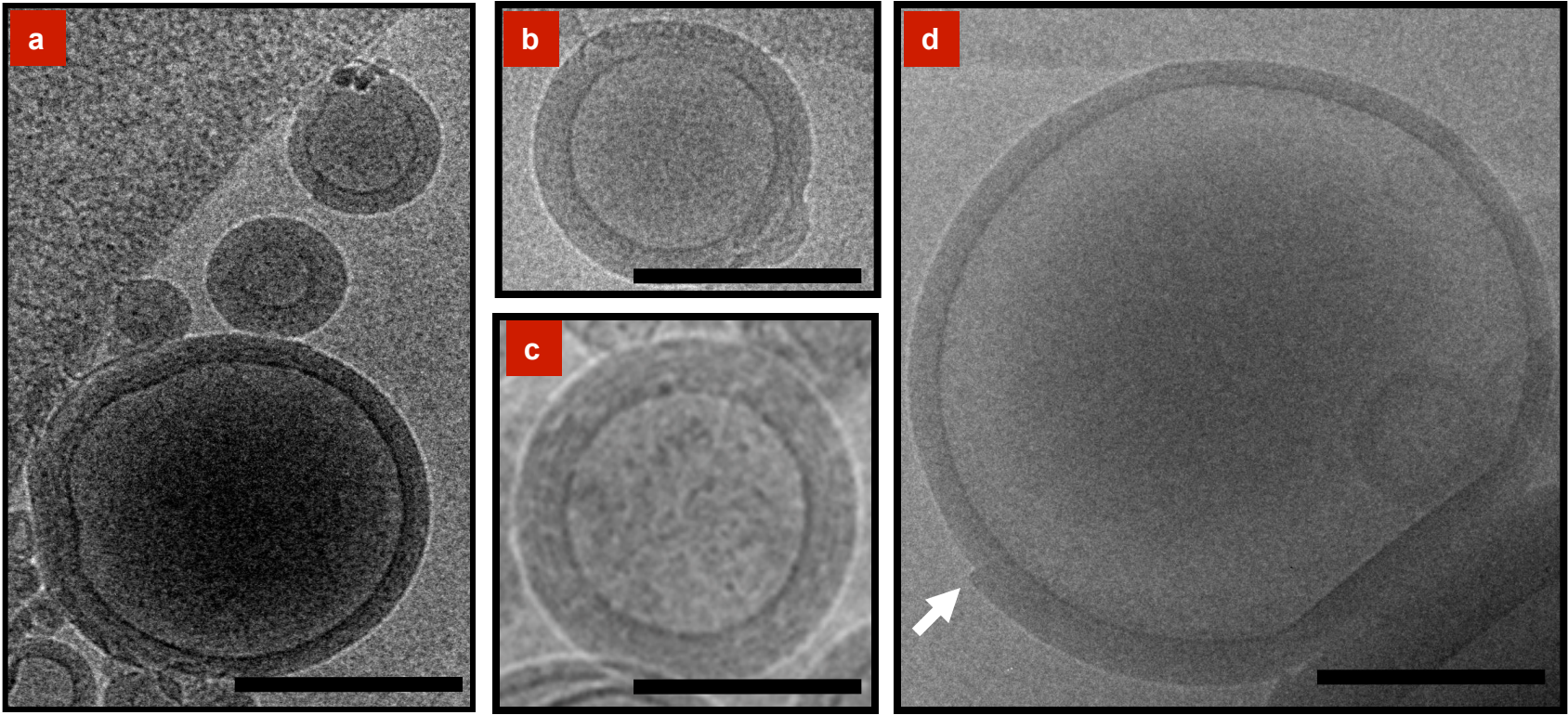
a



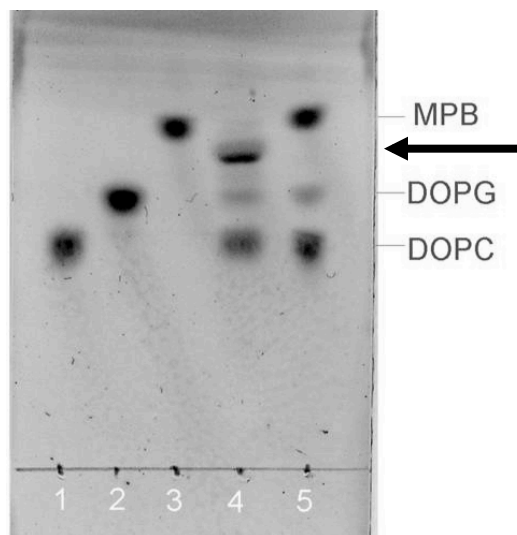
b



Sup. Fig. 2

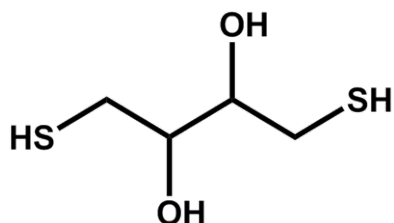


Sup. Fig. 3



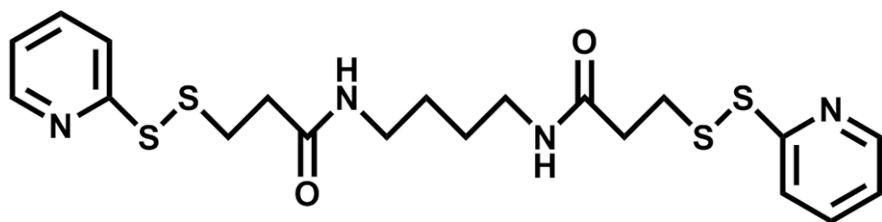
1. DOPC lipid alone
2. DOPG lipid alone
3. MPB lipid alone
4. MLVs following DTT crosslinking (ICMVs)
5. MLVs

Sup. Fig. 4



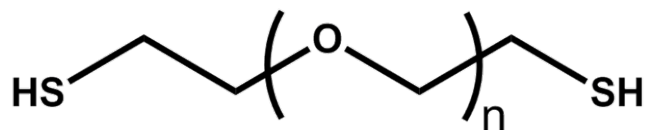
DTT (dithiothreitol)

MW 154



DPDPB (1,4-Di-[3'-(2'-pyridyldithio)-propionamido]butane)

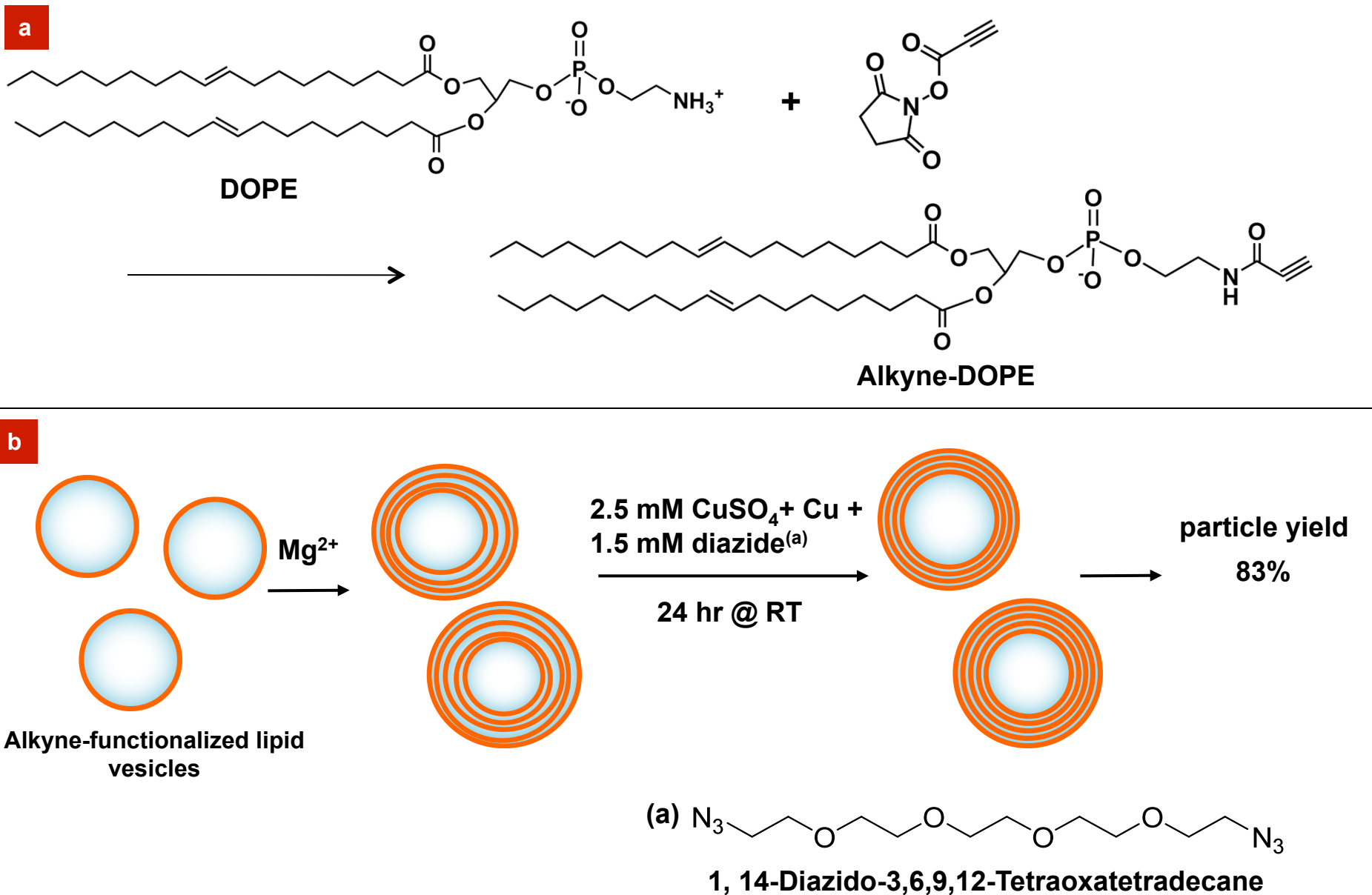
MW 483



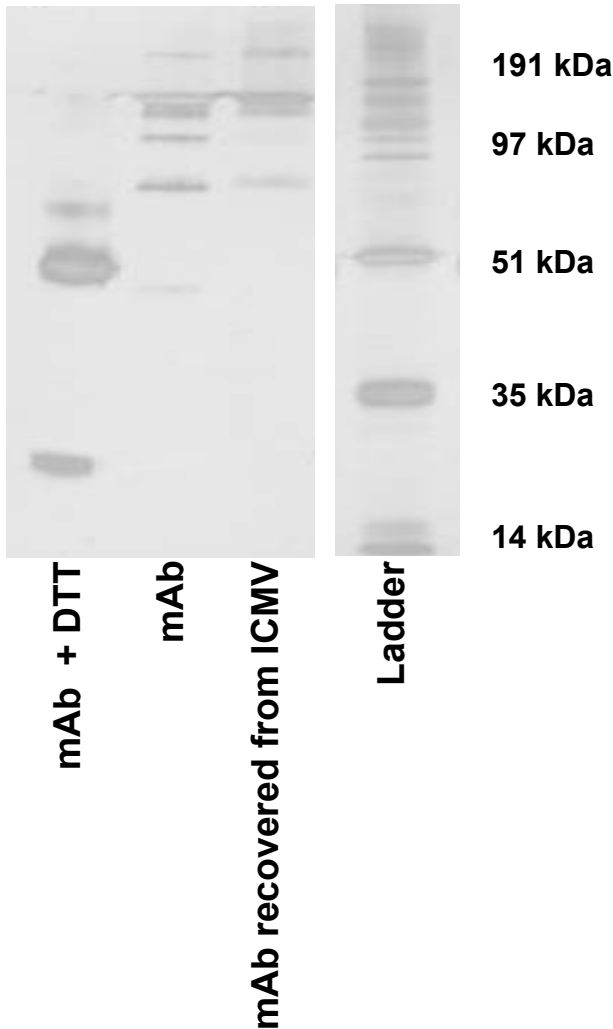
SH-PEG-SH (Polyethylene glycol dithiol)

MW 2000

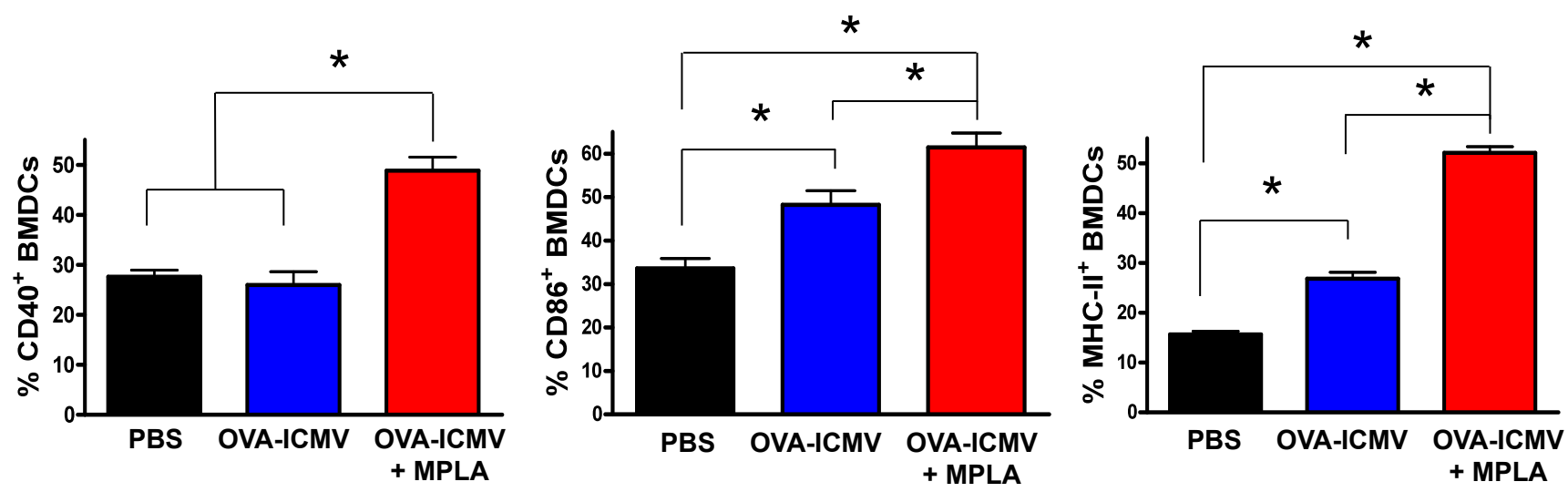
Sup. Fig. 5



Sup. Fig. 6



Sup. Fig. 7



Sup. Fig. 8

